



# Effect of azelaic acid on microstructure evolution and electrical properties of anodic aluminum foil for electrolytic capacitor

Sining Pan<sup>1,2,3,\*</sup> , Libo Liang<sup>1,\*</sup>, Baolin Lu<sup>1</sup>, Huibin Li<sup>1</sup>, and Yaowei Li<sup>1</sup>

<sup>1</sup> Postdoctoral Research Center, Guangxi Hezhou Guidong Electronics Technology Co. Ltd. Inc., Hezhou, China

<sup>2</sup> College of Artificial Intelligence, Hezhou University, Hezhou, China

<sup>3</sup> College of Chemistry and Bioengineering, Guilin University of Technology, Guilin, China

Received: 11 May 2020

Accepted: 1 December 2020

Published online:

1 January 2021

© The Author(s), under exclusive licence to Springer Science+Business Media, LLC part of Springer Nature 2021

## ABSTRACT

The effect of azelaic acid on microstructure evolution and electrical properties of anodic aluminum foil for electrolytic capacitor is studied quantitatively. The azelaic acid is selected as formation solution in the multi-step anodization process, and boric acid is applied for comparison. The field-emission scanning electron microscopy and X-ray diffractometer technologies are used for observation of microstructure and detection of crystallinity, respectively. The electrical properties are tested by LCR meter and T–V tester. The microstructure observation shows that the ‘corn-flake’ structures are taken place by ‘cotton-ball’ ones gradually along with the preparation process, and such phenomenon is more obvious when azelaic acid is used. The pores area of anodic aluminum foil formed in azelaic acid is larger because of the stronger acidity. The formation with azelaic acid induces smaller thickness of oxide film, promotes the formation of crystalline oxide, therefore, a barrier film with higher crystallinity and larger grain size is obtained. The barrier film formed in azelaic acid shows larger specific capacitance, lower withstand voltage and larger leakage current, which needs the multi-step anodization for performance improvement.

## 1 Introduction

Aluminum electrolytic capacitors are widely used in all types of electronic equipment [1–3]. Served as the working medium of aluminum electrolytic capacitor, the dielectric oxide film of anodic aluminum foil is grown on the surface through the multi-step anodization technology, including hydration,

anodization (which is also called formation), heat treatment and so on. The electrochemical etching and tunnel-widening technologies are applied for the production of anodic aluminum foil with high surface area [4–6]. The characteristics of oxide film affect the electrical performance of electrolytic capacitor directly. Depending on the anodization conditions, either amorphous or crystalline oxide can be obtained

Address correspondence to E-mail: supereve122@163.com; lianglibo321@163.com

[7]. One of the most important influence on the microstructure is the solution used in the formation process [8]. The crystalline form is mainly considered to be the dense  $\gamma$ - $\text{Al}_2\text{O}_3$  or  $\gamma'$ - $\text{Al}_2\text{O}_3$  layer, which contributes to the higher withstand voltage and larger specific capacitance [9]. Therefore, it is helpful to study the effect of formation solution on microstructure evolution and electrical properties of anodic aluminum foil, especially the structure and formation mechanism of oxide film, in order for the process improvement.

Since the formation solution has an significant influence on the microstructure and properties of anodic aluminum foil, researchers have carried out lots of work on it in recent years [10–13]. The most commonly used solution is boric acid, and the multi-step anodization process with the boric acid solution is widely applied [14]. Takahashi et al. [15] studied the effects of  $\text{SiO}_4^{4-}$ ,  $\text{PO}_4^{3-}$  and citric acid on the formation mechanism of the oxide film. The results showed that both the oxidation of aluminum and the formation of hydroxide films were retarded with increasing anion concentration in silicate and phosphate solutions. However, in citrate solutions, the oxidation rate increased, but the film formation rate decreased. Ban et al. [16, 17] studied the effect of citric acid and tartaric acid on the microstructure and electrochemical characteristics of anodic aluminum film. They found that the addition of citric acid and tartaric acid effectively promoted crystalline oxide formation and obtained a barrier film with a high degree of crystallinity. Sepúlveda et al. [18] investigated the growth behavior of anodic porous alumina formed on aluminum by anodizing in etidronic acid, and the influence of electrolyte temperature and anodizing time was studied with the averaged regularity ratio evaluated from Fast Fourier Transform intensity profile.

Generally, the solution system is divided into two kinds: inorganic acid and organic acid. The most typical representative of inorganic acid system is boric acid, and the azelaic acid is considered as the representative of organic acid system. Since the anodization process by the inorganic acid and organic acid has been widely applied for the manufacture of anodic aluminum foil, however, the quantitative comparison has received insufficient attention, especially from the point of microstructure evolution. In addition, detailed knowledge of the formation mechanism in the azelaic acid, as well as

the microstructure and electrical properties of oxide film is still required.

In this paper, the main objective is to investigate the effect of azelaic acid on microstructure evolution and electrical properties of anodic aluminum foil. The azelaic acid is used as the formation solution in the multi-step anodization process, and boric acid is applied for comparison. The microstructure observation and crystallinity detection are conducted by FE-SEM and XRD methods, respectively. The pores area and thickness of oxide film are measured based on the FE-SEM micrograph, while the grain size is calculated based on the XRD results. The electrical properties, such as the specific capacitance, withstand voltage, arrival time and leakage current, are also tested and discussed.

## 2 Experimental procedure

### 2.1 Sample preparation

The tunnel-etched aluminum foil with the thickness of 115  $\mu\text{m}$  and the surface area of  $50 \times 50 \text{ mm}^2$  is used as the specimen, as demonstrated in Fig. 1, which is with high purity and cubicity texture. The anodic aluminum foil is produced by the multi-step anodization process, and the schematic diagram is shown in Fig. 2. In addition, the detailed information of preparation process are listed in Table 1 and Table 2, respectively. The voltage used during the 'Formation I' stage is 330 V, while 550 V is applied in

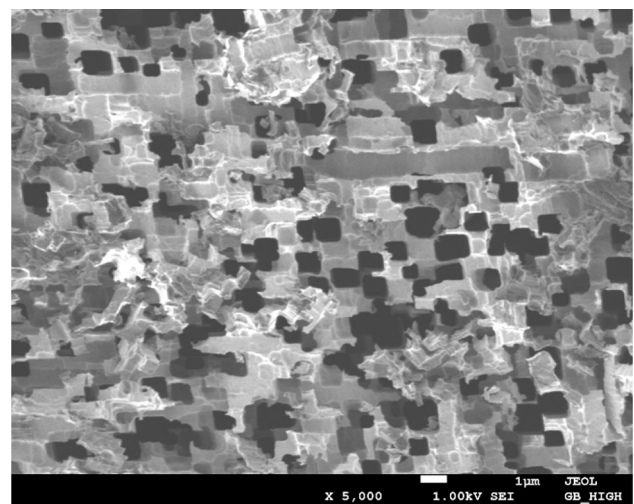


Fig. 1 Surface morphology of etched aluminum foil

the ‘Formation II’, ‘Formation III’, ‘Formation IV’ and ‘Formation V’ stage.

## 2.2 Microstructure characterization

The microstructure of aluminum foil is observed with field-emission scanning electron microscopy (FE-SEM, JEOL, JSM-6700F). The pores area is calculated based on the FE-SEM images. Before FE-SEM observation, the specimens are gold-sputtered for better observation condition, including the surface and cross-sectional specimens. The crystallographic structure is detected by an X-ray diffractometer (Ultima IV) with copper (Cu) anode, which operates at 40 kV and 40 mA. The 2-Theta scans are ranged from 10° to 80°, which are measured under the continuous mode with 0.02° step size and the scan speed of 10° per minute.

## 2.3 Measurement of electrical properties

The specific capacitance is measured by LCR meter in 80 g/L  $\text{NH}_4\text{B}_5\text{O}_8 \cdot 4\text{H}_2\text{O}$  at 30 °C and 120 Hz. A pure aluminum sheet is used as the counter electrode. The withstanding voltage, arrival time and leakage current, are tested by T-V tester (Model: TV1500V-3, Maker: Tenghao Electronic). The formed foils are charged with a nominal constant current density of  $i_a = 0.2 \text{ mA cm}^{-2}$  for 70 s in 70 g/L  $\text{H}_3\text{BO}_4$  solution at

85 °C. As soon as the current is applied, the voltage increases immediately, and then reaches a saturated value gradually. The change of cell voltage with time ( $V$  vs  $t$ ) is recorded. The arrival time  $T_r$  of anodic aluminum foil is defined as the time from power on until the voltage rises to 90% of rated voltage for anodic aluminum foil. The withstanding voltage of anodic aluminum foil is defined as the achieved voltage at 180 s after the arrival time  $T_r$ .

Under the constant-voltage condition, the current of anodic aluminum foil decreases gradually with the increase of time. However, the current would not decrease to zero but reaches a relatively stable state after dropping to a small value, and the current value corresponding to this stable state is called the leakage current  $I_\zeta$ .

## 3 Results and discussion

### 3.1 Effect of azelaic acid on microstructure

The surface micrographs of anodic aluminum foil are presented in Fig. 3, and the magnification of petal structure is inserted in each figure. The hydrous oxide film is shown in Fig. 3a, which is immersed in deionized water at 90 °C for 10 min. It is shown that the ‘corn-flake’ structures (which are the crystalline hydrous oxide  $[\text{AlO}(\text{OH})]$  [19]), are formed after hydration, which increases the blocked probability of tunnel pore. After the ‘Formation I’ stage (Fig. 3b and c) in boric acid of different concentration, marked with B-3# and A-3#, respectively, the ‘corn-flake’ structures are refined and flower-like, which promotes the blockage of tunnel pore. The surface morphology changes significantly after the later formation under higher voltage, heat treatment with high temperature and PD treatment. The ‘corn-flake’ structures are gradually taken place by ‘cotton-ball’ ones, as can be seen in Fig. 3d and f in boric acid, Fig. 3e and g in azelaic acid, respectively. Due to the structure transformation, the microstructure damage of petal structure is observed during preparation process. The structure transformation from ‘corn-flake’ to ‘cotton-ball’ is more obvious in azelaic acid. However, a few ‘corn-flake’ structures produced in the ‘Hydration’ stage is still preserved in the final sample, as shown in Fig. 3h and i.

From the inserted picture in Fig. 3, it is seen that the length of petal structure increases along with the

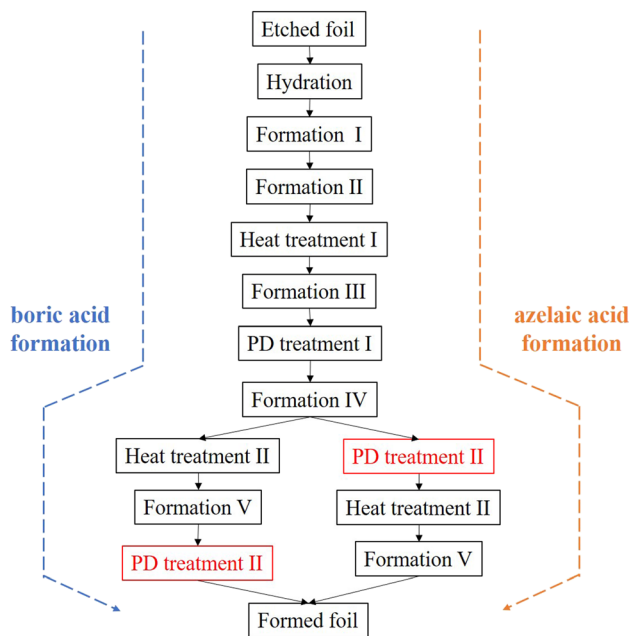


**Fig. 2** Preparation process

**Table 1** The detailed process for boric acid formation

Sample no.	Process	Temperature (°C)	Time (min)	Solution
B-1#	Etched foil	–	–	–
B-2#	Hydration	90	10	Deionized water
B-3#	Formation I	90	15	3% boric acid (pH 4.0–4.5)
B-4#	Formation II	90	30	6% boric acid (pH 5.3–5.8)
B-5#	Heat treatment I	500	5	–
B-6#	Formation III	90	10	6% boric acid (pH 5.3–5.8)
B-7#	PD treatment I	60	10	1.5% phosphoric acid
B-8#	Formation IV	90	10	6% boric acid (pH 5.3–5.8)
B-9#	Heat treatment II	500	5	–
B-10#	Formation V	90	10	6% boric acid (pH 5.3–5.8)
B-11#	PD treatment II	40	10	0.2% phosphoric acid
B-12#	Formed foil	300	5	–

**Table 2** The detailed process for azelaic acid formation

Sample no.	Process	Temperature (°C)	Time (min)	Solution
A-1#	Etched foil	–	–	–
A-2#	Hydration	90	10	Deionized water
A-3#	Formation I	90	15	0.3% boric acid (pH 4.0–4.5)
A-4#	Formation II	90	30	0.03% azelaic acid (pH 4.7–5.3)
A-5#	Heat treatment I	500	5	–
A-6#	Formation III	90	10	0.03% azelaic acid (pH 4.7–5.3)
A-7#	PD treatment I	60	10	1.5% phosphoric acid
A-8#	Formation IV	90	10	0.03% azelaic acid (pH 4.7–5.3)
A-9#	PD treatment II	60	5	0.2% phosphoric acid
A-10#	Heat treatment II	300	5	–
A-11#	Formation V	90	10	0.03% azelaic acid (pH 4.7–5.3)
A-12#	Formed foil	300	5	–

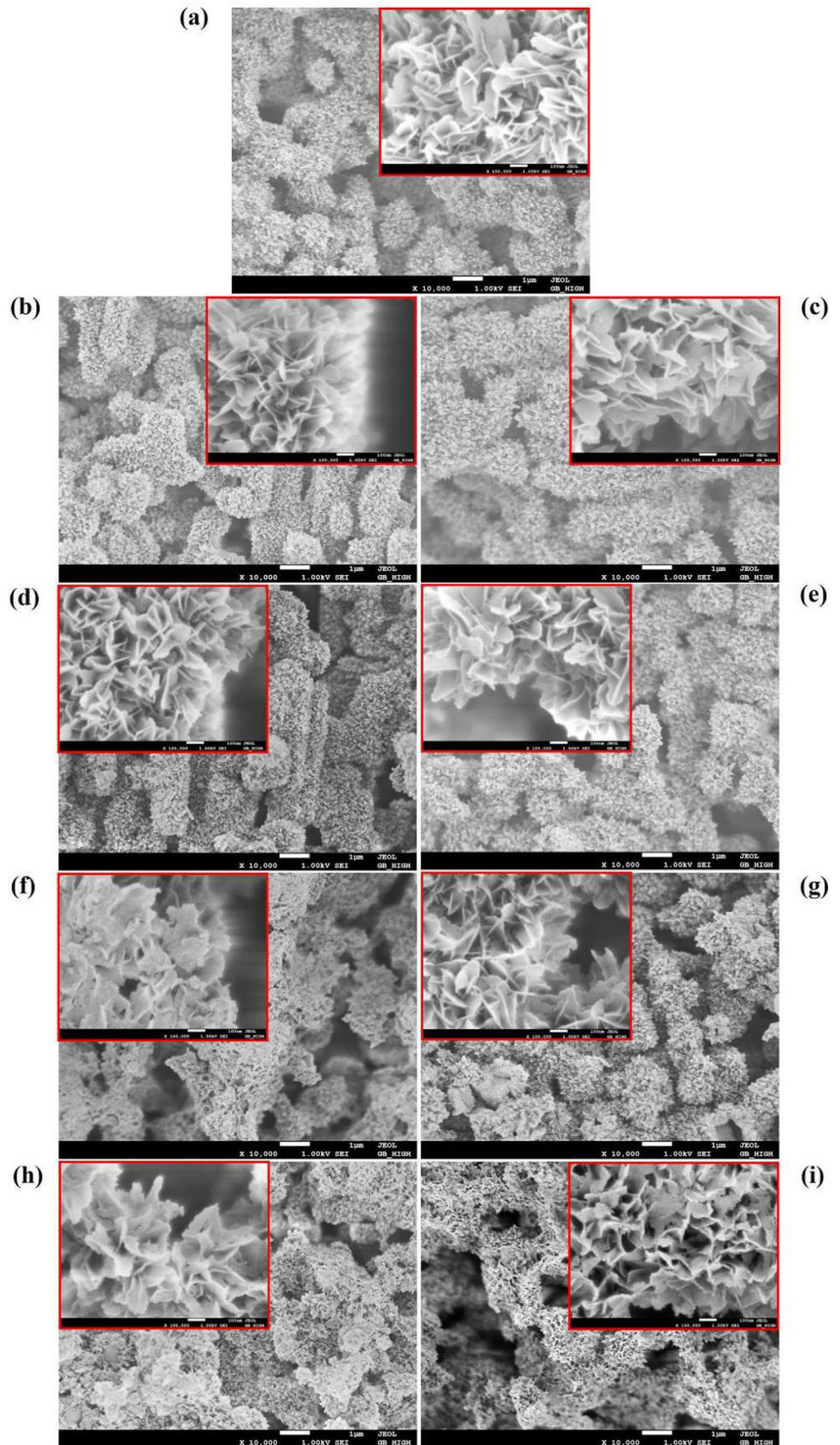
preparation process, ranging from 60–120 to 100–140 nm. At the same time, the damage of petal structure is observed during the preparation process. As listed in Tables 1 and 2, azelaic acid is more acidic than boric acid. Therefore, the azelaic acid has a high selective solubility to the oxide film during anodization, and introduces more micro defects, such as gaps and voids [16, 17]. Crystal transformation will take place during the formation process. At this time, the volume occupied by oxide film remains unchanged (so the thickness is almost constant). However, the density of amorphous oxide film and  $\gamma$ -Al<sub>2</sub>O<sub>3</sub> is about 3.0 g/cm<sup>3</sup> and 3.5 g/cm<sup>3</sup>, respectively. Therefore, the volume shrinks during the transformation, and many voids are produced. The void is filled with O<sub>2</sub>, a byproduct of anode reaction, and there are micro cracks connected with the solution outside. When the current is cut off after formation, O<sub>2</sub> in the void is discharged, and the solution is inhaled, causing hydrolysis degradation of oxide film. And

then, the formation is carried out again with a small current, and the Al<sub>2</sub>O<sub>3</sub> formed by the re-oxidation can effectively repair the voids.

In addition, the defects in the oxide film can also be effectively reduced by intermediate heat treatment between multi-step formation. It is because the original defects in the oxide film increase rapidly due to the different expansion coefficient under thermal action. After the next reformation, the crystallization process is almost over, and the new oxide film is formed at the crack to be filled. The defects in the oxide film are reduced and tend to be uniform. Therefore, the production process including multiple formations, multiple heat treatment and multiple “PD treatment”, are applied for the preparation of anodic aluminum foil in this research.

The partial dissolution of hydrated oxide film caused by phosphoric acid is perforation-type. In boric acid system, the last ‘PD treatment’ (B-11#) is after the final formation step (B-10#), and before the

**Fig. 3** FE-SEM micrograph of surface samples. **a** 2#, **b** B-3#, **d** B-4#, **f** B-8#, **h** B-12#, **c** A-3#, **e** A-4#, **g** A-8#, **i** A-12#



final drying step (B-12#), so the structural damage of perforated petals after 'PD treatment' is retained in the final sample, which can be seen in the inserted figure of Fig. 3h. However, in the azelaic acid system, the last 'PD treatment' (A-9#) is designed before the final formation step (A-11#). Therefore, the edge and inside of petal structure can be refined by the following heat treatment (A-10#) and formation (A-11#), as shown in the inserted figure of Fig. 3i.

To quantitatively compare the blocking of oxide film formed in a different solution to the tunnel hole, the pores area is calculated by using ImagePro software, which is based on the FE-SEM images. Firstly, the FE-SEM images are binarized. Then, the feature areas with pixel difference are filtered out and considered as the pores area (expressed in pixels). The pores area of sample 1# is selected as the initial normalized pores area, the normalized values of pores area for the other samples are calculated by the following equation[20]:

$$N_i' = \frac{N_i}{N_1}$$

where  $N_1$  is the pores area of sample 1#,  $N_i$  is the pores area of the objective sample, and  $N_i'$  is the normalized pores area for the objective sample.

The evolution of pores area is illustrated in Fig. 4. The pores area decreases after the stage of 'Hydration' (2#), 'Formation I' (3#), 'Formation II' (4#), 'Heat treatment I' (5#) and 'Formation III' (6#). It is noted that after 'PD treatment I' (7#), the pores area stops decreasing, and starts to increase, which means the pore blockage is relieved. During the following process, the pores area continues to decrease until the

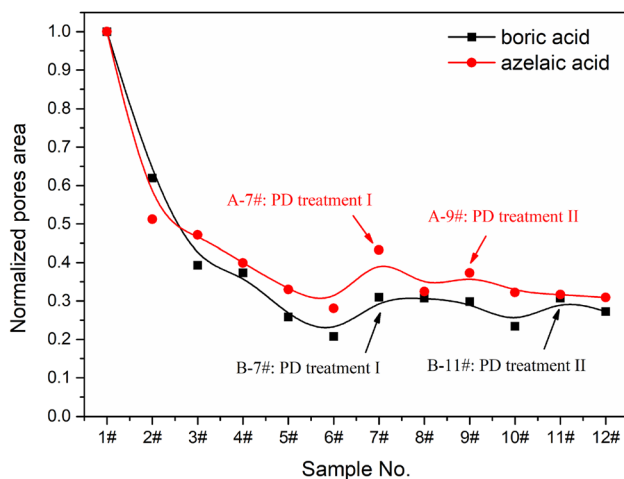


Fig. 4 Evolution of pores area

'PD treatment II' begins (B-11# and A-9#). From Fig. 4, the pores area in Al foil formed in azelaic acid is larger than that in boric acid. The acidity of azelaic acid is stronger, causing higher dissolving ability of oxide film. Therefore, the thickness of oxide film in azelaic acid becomes smaller, and the blockage of tunnel hole is reduced, making larger pores area.

The cross-sectional samples are displayed in Fig. 5. The oxide film of aluminum foil shows a two-layers structure, which is similar to other research [7]. The region located between the two red solid lines in Fig. 5 is defined as the inner layer, while the outer layer is referred to the region between the middle red solid line and the dotted yellow line. The structure of inner layer is similar to Pseudo BÖhmite  $\gamma\text{-Al}_2\text{O}_3 \cdot 2\text{H}_2\text{O}$ , which can be converted into  $\gamma\text{-Al}_2\text{O}_3$  easily in the following formation. The outer layer is fibrous, which is hard to transform into  $\gamma\text{-Al}_2\text{O}_3$  because of its large water content. In Fig. 5a, the thickness of inner layer and outer layer is about 100 nm and 370 nm, respectively, which is similar to other researches [7, 21]. During the subsequent formation, phosphoric acid treatment and heat treatment, as shown in the other images of Fig. 5, barrier oxide is obtained between the aluminum and Pseudo BÖhmite film. The thickness of both the inner layer and outer layer changes significantly. It is shown in Fig. 5b–g that, the thickness of dense inner layer increases gradually, however, the thickness of fibrous outer layer decreases. Such changes are more obvious in azelaic acid than that in boric acid.

The evolutionary curve of oxide thickness is demonstrated in Fig. 6. Three different positions are selected, and the average is measured and used for comparison. The thickness of petal structure in outer layer decreases in the whole process, which is shown in Fig. 6a. However, the decreasing tendency is more significant in azelaic acid than that in boric acid. After the 'Hydration' stage, the initial thickness of petal structure is about 370 nm. The final thickness of petal structure in boric acid and azelaic acid is 130 nm and 110 nm, respectively.

In contrast, during the preparation process, the thickness of dense inner layer increases, as shown in Fig. 6b. It is noted that, in boric acid, the thickness of dense inner layer increases significantly from the 100 nm (B-2#) to about 530 nm after the 'Formation II' stage (B-4#), and keeps increasing to 570 nm until the end of preparation process. Similarly, in azelaic acid, the thickness of dense inner layer increases greatly

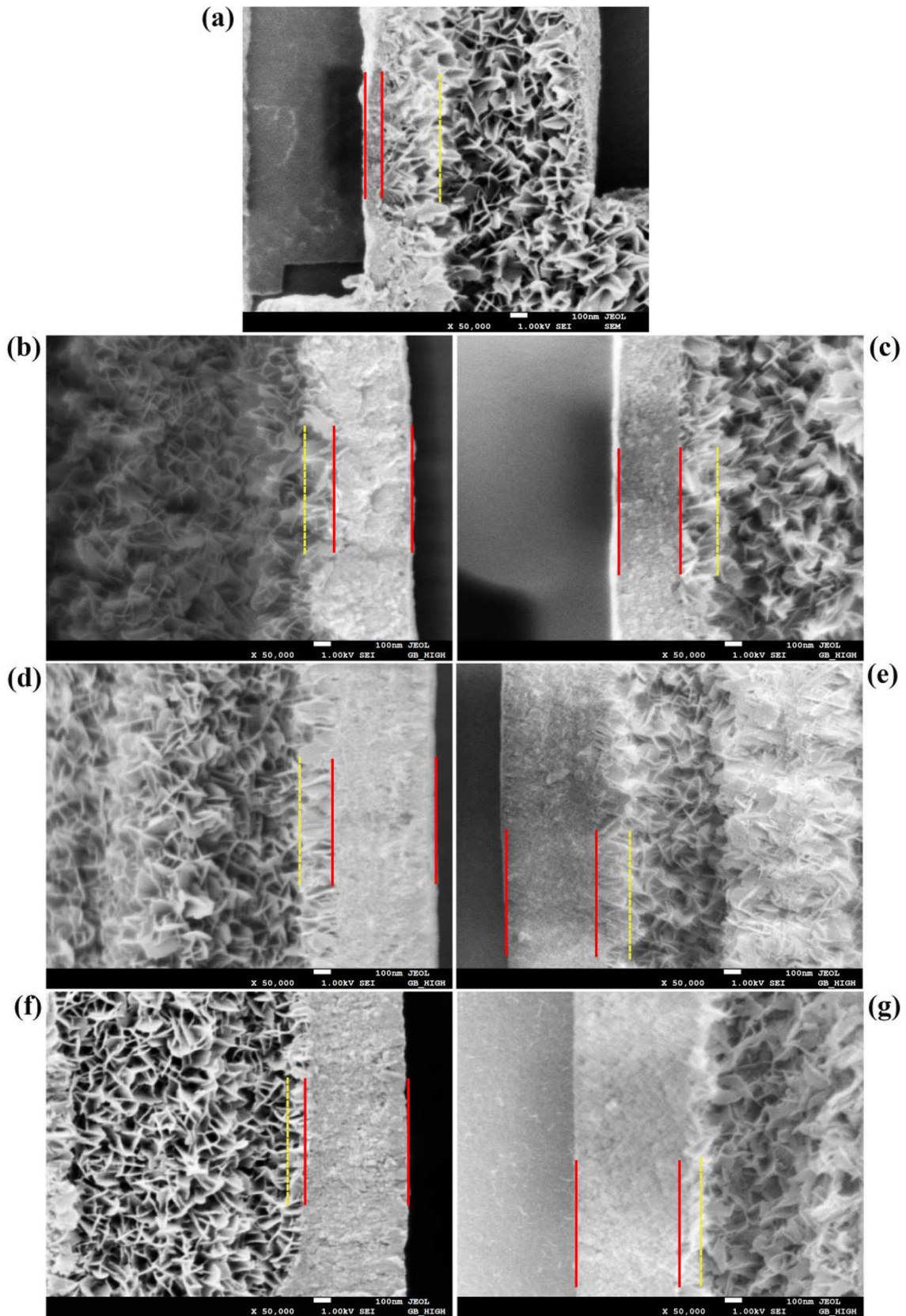


**Fig. 5** FE-SEM micrograph of cross-sectional samples. **a** 2#, **b** B-3#, **d** B-4#, **f** B-12#, **c** A-3#, **e** A-4#, **g** A-12#

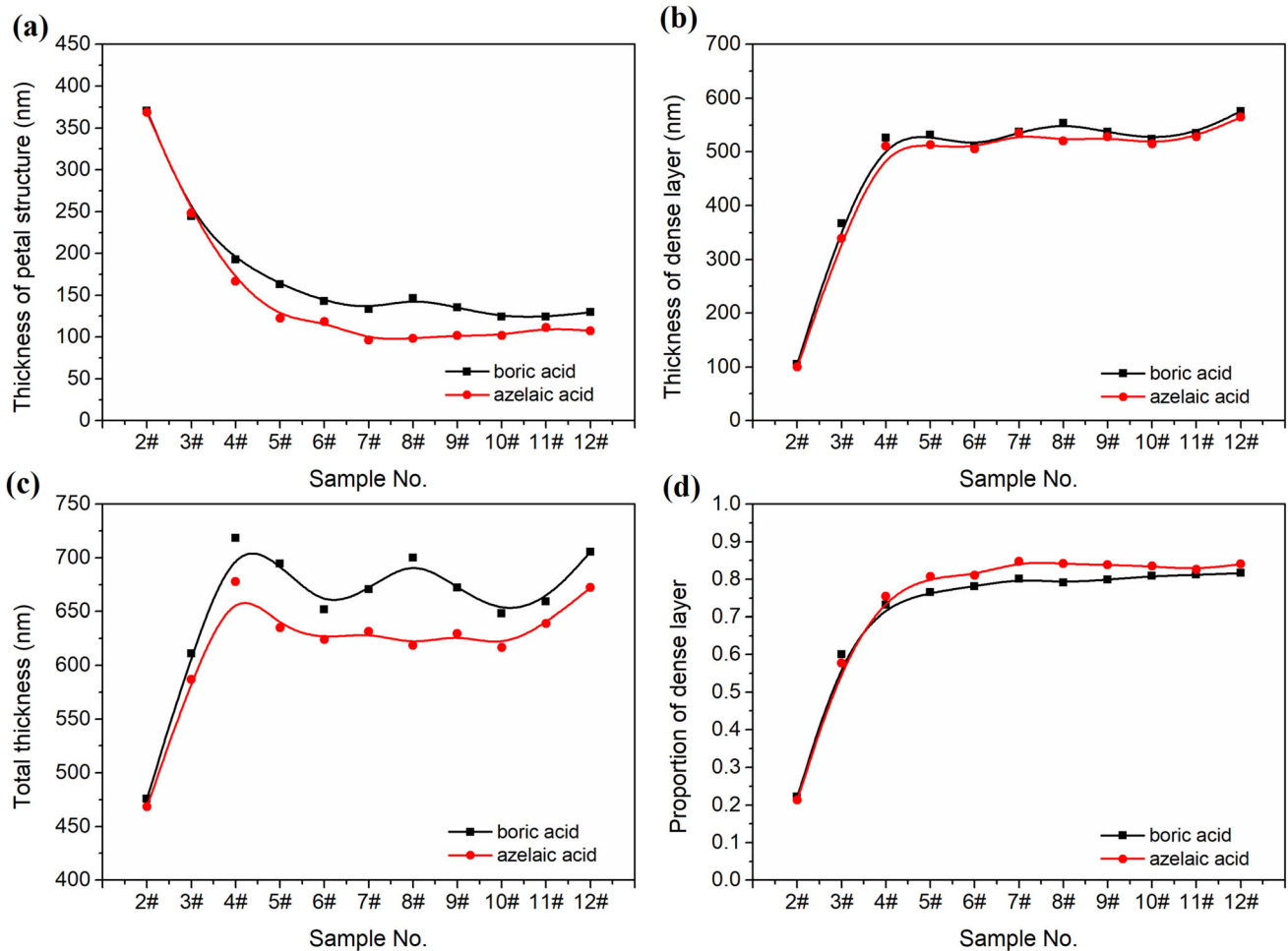


**Fig. 6** Thickness evolution of oxide layer. **a** The thickness of petal structure, **b** the thickness of dense layer, **c** total thickness, **d** the proportion of dense layer

from 100 nm (A-2#) to about 520 nm after the 'Formation II' stage (A-4#), and keeps increasing to the final 560 nm.

As shown in Fig. 6c, the total thickness of oxide film in azelaic acid is always smaller than that in boric acid, reflecting the effect of formation solution on the microstructure. The final value of total thickness is 700 nm and 670 nm, respectively. The ionization constants of boric acid and azelaic acid is  $5.8 \times 10^{-10}$  and  $2.82 \times 10^{-5}$ , respectively, which shows that the acidity of azelaic acid is stronger than boric acid. The solution with stronger acidity will dissolve more oxide film in the anodization process, which induces thinner thickness of oxide film.

The fibrous outer layer of oxide film and the residual undehydrated hydrated oxide film are unfavorable, which are easy to block the micro tunnel holes, causes the specific capacitance damaged. The

dense  $\gamma$ - $\text{Al}_2\text{O}_3$  or  $\gamma'$ - $\text{Al}_2\text{O}_3$  film is the main working medium, which significantly affects the withstand voltage and specific capacitance [1]. The thickness proportion of dense layer is calculated and demonstrated in Fig. 6d. It is obvious that the proportion of dense layer is larger in azelaic acid than that in boric acid, which means that the azelaic acid can promote crystal transformation in the dense layer. The thickness of oxide film is proportional to the voltage during anodization process [22]. According to the definition of withstand voltage thickness per volt  $D = d/V_f$ , where  $d$  is the thickness of dense inner layer, and  $V_f$  is the formation voltage ( $V_f = 550\text{V}$  in this situation). Therefore, the withstand thickness per volt of the films formed in boric acid and azelaic acid is calculated as 1.036 nm/V and 1.018 nm/V, respectively. The withstand voltage thickness per volt of the amorphous oxide film and  $\gamma'$ - $\text{Al}_2\text{O}_3$  is about 1.3



nm/V and 0.9 nm/V, respectively, however, that of the crystalline composite oxide film is between them. The smaller the withstand voltage thickness is, the higher the specific capacitance is. It can be concluded that the specific capacitance of anodic aluminum foil formed in azelaic acid will be larger.

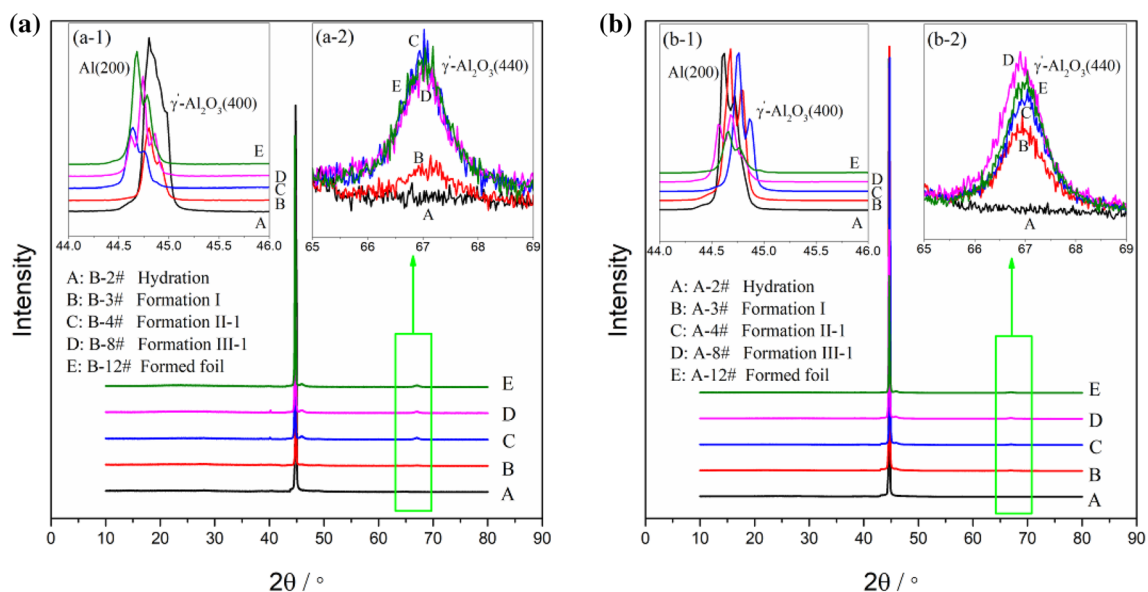
### 3.2 Effect of azelaic acid on crystallinity

Figure 7 shows the XRD curves of aluminum foil during preparation process. The strongest peak corresponds to Al (200), and other distinct peaks correspond to crystalline oxide in barrier films, marked by  $\gamma'$ -Al<sub>2</sub>O<sub>3</sub> (400) and  $\gamma'$ -Al<sub>2</sub>O<sub>3</sub> (440). Due to the similar diffraction angle, the Al (200) peak and  $\gamma'$ -Al<sub>2</sub>O<sub>3</sub> (400) peak seem coincided, which can be observed in Fig. 7a-1 and b-1. However, the coincidence degree of the two diffraction peaks is different. The coincidence degree in boric acid is higher than that in azelaic acid. Moreover, the intensity of diffraction peak  $\gamma'$ -Al<sub>2</sub>O<sub>3</sub> (440) increases gradually, as shown in Fig. 7a-2 and b-2, which means that the grain size is changing during preparation process. For boric acid, only the intensity of  $\gamma'$ -Al<sub>2</sub>O<sub>3</sub> (440) diffraction peak changes with preparation process. As for azelaic acid, both the intensity and diffraction angle of  $\gamma'$ -Al<sub>2</sub>O<sub>3</sub> (440) diffraction peak change during preparation process.

The grain size is calculated for quantitative characterization of crystallinity evolution. The calculation of grain size is based on the width of  $\gamma'$ -Al<sub>2</sub>O<sub>3</sub> (440)

peak and Scherrer formula. The calculated grain size of  $\gamma'$ -Al<sub>2</sub>O<sub>3</sub> is demonstrated in Fig. 8, showing a decreasing tendency. The grain size is about 25 nm after the 'Hydration' stage. For boric acid, the grain size reduces sharply to below 15 nm once the formation begins. Such decrease keeps until the end, and 10 nm is obtained finally. However, for azelaic acid, the grain size decreases greatly to about 13 nm when the formation begins, and keeps such value during the following process.

The final larger grain obtained by azelaic acid means crystallinity improvement of oxide film. The stronger the acidity of formation solution, the higher the selective solubility of oxide film during anodization process. The oxide film with high crystallinity has stronger corrosion resistance than that with low crystallinity, therefore, the oxide with low crystallinity preferentially dissolves and loses the ability of voltage resistance [16]. As a result, the formation speed of oxide film decreases, and it will take a long formation time to withstand 550V during formation. The long time under high electric field helps to improve the overall crystallinity of oxide film. The transformation process of Al →  $\gamma'$ -Al<sub>2</sub>O<sub>3</sub> in the inner layer and that of AlOOH·H<sub>2</sub>O →  $\gamma'$ -Al<sub>2</sub>O<sub>3</sub> in the outer layer are intensified, which induces high crystallinity of oxide film and increase of grain size.



**Fig. 7** XRD curves of aluminum foil. **a** Boric acid, **b** azelaic acid

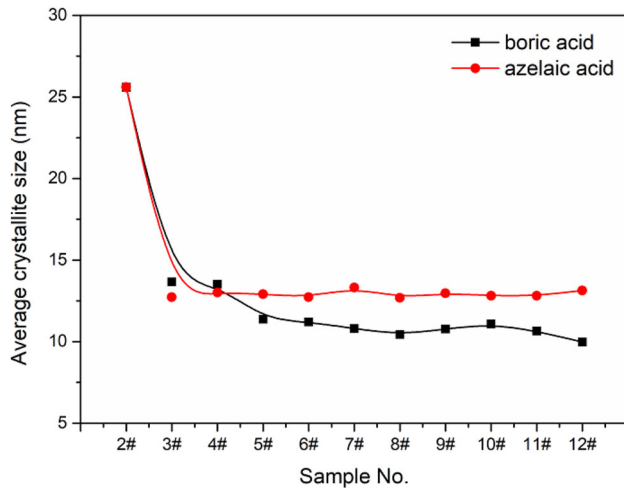


**Fig. 8** Evolution of  $\gamma'$ - $\text{Al}_2\text{O}_3$  grain size

### 3.3 Effect of azelaic acid on electrical properties

In different formation solutions, the oxide film with different structure can be produced, such as amorphous and crystalline. The surface of oxide film will be mixed with considerable amounts of anions in the formation solution, resulting in different chemical stability of anodic aluminum foil formed in different formation solutions. The electrical properties of anodic aluminum foil are measured and listed in Table 3. The specific capacitance of films produced by boric acid (B-12#) is lower than that in azelaic acid (A-12#). According to the electrostatic capacity formula of parallel plate capacitor,  $C = \epsilon_0 \epsilon_s / d$ , where  $\epsilon_0$  is vacuum dielectric constant ( $\epsilon_0 = 8.85 \times 10^{-12}$  F/m),  $\epsilon$  is the relative dielectric constant,  $s$  is the surface area,  $d$  is the thickness of oxide film. Since the acidity of azelaic acid is stronger, the crystallinity of anodic oxide film is improved, and the relative dielectric constant  $\epsilon$  is increased greatly. In addition, the thickness of oxide film formed in azelaic acid is smaller, making the blockage of tunnel hole reduced, thus increasing the surface area of aluminum foil. The above factors are contributed to the larger specific capacitance of films produced by azelaic acid.

As shown in Table 3, the arrival time  $T_r$  of aluminum foil is the same, however, the withstand

voltage  $V_t$  in boric acid is higher, and the related rising speed to  $V_t$  is higher.  $V_t$  and rising speed are indirect reflections of micro defects in the oxide film. One part of the current is used to repair inherent defects in the oxide film, and the other part is used to improve the formation of new oxide film and the withstand voltage. The higher the defect density in the oxide film, the slower the rising speed and the lower  $V_t$ . The azelaic acid induces high crystallinity, at the same time, it also causes the phase transformation shrinkage and increases the internal stress, which produces the gap defects on the interface of aluminum oxide film. The defects will affect the service life and stability of electrolytic capacitor, which requires multi-step repair of oxide film [16, 17].

Although the anodized film is an insulator with high electric field strength, it is not a perfect ultra-thin film, and there are various tiny defects, cavities and gaps on the surface. The leakage current  $I_\zeta$  is composed of impurity ions and electron current passing through these defects. Since the formation condition of oxide film is closely related to defects, the formation solution does have a great influence on leakage current  $I_\zeta$ . More defects are induced in azelaic acid, therefore, larger  $I_\zeta$  is expected, as listed in Table 3.

## 4 Conclusions

The effect of azelaic acid on the microstructure evolution and electrical properties of anodic aluminum foil is investigated quantitatively. The formation with boric acid is conducted for comparison with the effect of azelaic acid. The 'corn-flake' structure, which is crystalline hydrous oxide [ $\text{AlO}(\text{OH})$ ], is gradually taken place by 'cotton-ball' structure along with the preparation process, and such phenomenon is more obvious when azelaic acid is used. The azelaic acid with stronger acidity will dissolve more oxide film during anodization process, which induces larger pores area and smaller thickness of oxide film. In addition, the azelaic acid helps to promote the

**Table 3** Electrical properties of anodic aluminum foil

Sample No.	Specific capacitance ( $\mu\text{F cm}^{-2}$ )	$V_t$ (V)	$T_r$ (s)	$I_\zeta$ ( $\mu\text{A}$ )
B-12#	0.728	561	140	60
A-12#	0.754	546	140	93

formation of crystalline oxide, obtain barrier film with higher crystallinity and larger grain size. The barrier film formed in azelaic acid is rich in defects at its outer layer from the transformation of Pseudo Böhmite to  $\gamma'$ -Al<sub>2</sub>O<sub>3</sub>. The barrier film formed in azelaic acid shows larger specific capacitance, lower withstand voltage and larger leakage current. Therefore, it is necessary to repair the defects with multi-step anodization to improve overall performance of anodic aluminum foil.

## Acknowledgements

This research was supported by the Project fund by China Postdoctoral Science Foundation (2019M663871XB), Postdoctoral Science Foundation of Guangxi Province of China, the Major scientific and technological projects of Guangxi Province of China (AA17202004), and the Innovation-driven Development Project of Hezhou City (ZX1907001).

## References

- Z.S. Feng, J.J. Chen, C. Zhang, N. Zhao, Z. Liang, *Ceram. Int.* **38**, 2501 (2012)
- F. Chen, S.S. Park, *ECS J. Solid State Sc.* **4**, 293 (2015)
- L. Xiang, S.S. Park, *Key Eng. Mater.* **737**, 143 (2017)
- L. Liang, Y. He, H. Song, X. Yang, X. Cai, C. Xiong, Y. Li, *Corros. Sci.* **70**, 180 (2013)
- L. Liang, Y. He, H. Song, X. Yang, X. Cai, *Corros. Sci.* **79**, 21 (2014)
- G. Scaduto, M. Santamaria, P. Bocchetta, F. Di Quarto, *Thin Solid Films* **550**, 128 (2014)
- H. Uchi, T. Kanno, R.S. Alwitt, *J. Electrochem. Soc.* **148**, 17 (2001)
- J. Chang, C. Liao, C. Chen, W. Tsai, *J. Power Sources* **138**, 301 (2004)
- A.C. Geiculescu, T.F. Strange, *Thin Solid Films* **503**, 45 (2006)
- I. Vrublevsky, V. Parkoun, J. Schreckenbach, W.A. Goedel, *Appl. Surf. Sci.* **252**, 5100 (2006)
- N. Hassanzadeh, H. Omidvar, M. Poorbafrani, S.H. Tabaian, *Arab. J. Sci. Eng.* **38**, 1305 (2013)
- T. Kikuchi, T. Yamamoto, S. Natsui, R.O. Suzuki, *Electrochim. Acta* **123**, 14 (2014)
- R.A. Mirzoev, A.D. Davydov, D.K. Kurmyalevskaya, A.N. Bazylyk, S.I. Vstupov, *Electrochim. Acta* **184**, 214 (2015)
- J. Lee, J.Y. Kim, J.K. Kim, J.H. Lee, H.Y. Chung, Y.S. Tak, *Corros. Sci.* **51**, 1501 (2009)
- H. Takahashi, M. Yamaki, R. Furuichi, *Corros. Sci.* **31**, 243 (1990)
- C. Ban, Y. He, X. Shao, *T. Nonferr. Metal. Soc.* **21**, 133 (2011)
- C. Ban, Y. He, X. Shao, *J. Mater. Sci. Mater. El.* **24**, 3442 (2013)
- M. Sepúlveda, J.G. Castaño, F. Echeverría, *Appl. Surf. Sci.* **454**, 210 (2018)
- A.C. Geiculescu, T.F. Strange, *Thin Solid Films* **445**, 105 (2003)
- S. Pan, L. Liang, B. Lu, H. Li, *J. Alloy. Compd.* **823**, 153795 (2020)
- C. Ban, F. Wang, J. Chen, Z. Liu, *J. Mater. Sci.-Mater. El.* **29**, 16166 (2018)
- R.S. Alwitt, C.K. Dyer, *Electrochim. Acta* **23**, 355 (1978)

**Publisher's Note** Springer Nature remains neutral with regard to jurisdictional claims in published maps and institutional affiliations.